CHAPTER 23

Instrumental evaluation of the deep water directional wave climate along the Mediterranean coast of Israel

Ya. A. Iosilevskii[1], D. S. Rosen[1], A. Golik[1], and D. L. Inman[2]

Abstract

The frequency-directional deep water wave climate along the Mediterranean coast of Israel was evaluated for the first time by computer numerical analysis using *instrumental shallow water measurements*. The shallow water data underlying the study were gathered within the period from 1984 through 1991 by two CAS (Cassette Acquisition System) wave measuring stations located off Haifa (North) and Ashkelon (South) along the Mediterranean coast of Israel. The paper includes a brief description of the data gathering, analysis, and processing methods, and it also includes main results of the study.

1. Introduction

It is both expensive and technically complicated to acquire accurate instrumental deep water data needed for computing the respective height, frequency, and direction of water waves. A quite cheap and commonly available practical way to evaluate frequency-directional spectra of water waves in deep water is to reconstruct those spectra from appropriate shallow water measurements. This approach is adopted in this study.

---

[1]National Institute of Oceanography: Israel Oceanographic and Limnological Research, Tel Shikmona P.O. Box 8030, Haifa 31080, Israel

[2]CCS, Scripps Institution of Oceanography, University of California, San Diego, La Jolla, Ca. 92093, U.S.A

In studying or simulating the wave climate in the offshore region, the coastal engineer typically employs the method which may be called '*the representative monochromatic wave method*'. In the framework of this method, the coastal engineer approximates the offshore irregular sea state by the corresponding *representative* (e.g., *characteristic*) *monochromatic wave*; and he investigates the refraction transformation of this monochromatic wave as it propagates shoreward. Although the representative monochromatic wave method is widely used in coastal engineering practice, the coastal engineer is usully unaware of the degree of accuracy of that method.

In contrast to the representative monochromatic wave method, the method of refraction transformation, which is used in this study, may be called '*the spectral decomposition method*'. It consists of three steps: (i) decomposition of the measured shallow water sea surface displacement from equilibrium into monochromatic wave components (say, by the FFT method); (ii) refraction transformation of each component; (iii) computation of the linear superposition of the component results. The spectral decomposition method is more consistent than the representative monochromatic wave method. Also, from the standpoint of both physical and numerical analysis, the latter method is a particular case of the former method. The two methods are compared in this study.

As contrasted to the evaluations of the present study, none of the previous wave climate evaluations at the Mediterranean coast of Israel, which were reported by Rosen & Kit (1981), Goldsmith & Sofer (1982), Rosen (1982), Carmel *et al* (1985b), had the property to be directional, deep water, and instrumental all together.

The term '*wave weather*', as contrasted to '*wave climate*', is used in this paper interchangeably with the presently common term '*sea state*'. The term '*shallow water*' is used as a class synonym of the term '*not deep water*'.

2. Data gathering

The row data used in this study were collected by two similar CAS (Cassette Acquisition System - see Boyd & Lowe (1985)) wave measuring stations located off Haifa (North) and Ashkelon (South) along the Mediterranean coast of Israel. Each station is composed of a linear array of three pressure gauges with spacings of 12 m and 24 m between two successive gauges. Both arrays are installed at a mean depth of 8.5 m, 0.95 m above the sea bottom. Consequently, the wind water waves of typical periods, say, from 4 sec. to 14 sec., i. e. of wavelengths from approximately 24 m to approximately 124 m at the station location, undergo *refraction* due to bathymetry effects before they reach the station.

The wave measuring station located at Ashkelon was intermittently operational from March 1984 through May 1987 and from August 1989 through February 1990. The wave measuring station located at Dado Beach, Haifa, was intermittently operational from March 1984 through April 1987 and from April 1989 through May 1991. Wave measurements have been carried out by each station for 34 min. 8 sec. every 6 hours, at a sampling rate of 2 Hz. A single whole phenomenon of the above duration when a CAS station samples with the rate of 2 Hz is said to be a *fast mode event* (briefly, an *FME*).

3. Physical and mathematical prerequisites

A description of the physical and mathematical concepts underlying the results reported in this paper is beyond its scope. Still, in order to discuss those results conveniently, we will make explicit some elementary physical and mathematical notions, - largely, by introducing the appropriate notation.

3.1. A coordinate system

A local working right-handed rectangular rectilinear coordinate system is chosen in such a way that its XY-plane coincides with the equilibrium sea surface, and its Z-axis is directed vertically upward. The origin of the coodinate system is located somewhere in deep water area, the X-axis is directed shoreward, and the Y-axis is, in a crude sense, parallel to the local shoreline.

3.2. General notation

's' and 'd' are subscript acronyms for 'shallow water' and 'deep water', respectively; '*' is a subscript ellipsis for 's' or 'd'; P_* is a point on the equilibrium sea surface; P_s is the shallow water point on the equilibrium sea surface under which the water wave measuring station is located; ρ is the mass density of sea water, (1028.8 kg/m^3); g is the acceleration of gravity (9.81 m/sec^2).

3.3. Parameters characterizing continuous spatiotemporal Fourier transform of the sea surface displacement equilibrium at the point P_*

ν = a monochromatic water wave frequency (Hz);

$\tau(\nu)$ = $1/\nu$ = the period of a monochromatic water wave of frequency ν (sec);

$\underset{\sim}{\varkappa}_*(\nu)$ = the propagation vector of a plane monochromatic water wave of frequency ν at P_* (m^{-1});

ϑ = the direction of $\underset{\sim}{\varkappa}_*(\nu)$ relative to the positive direction of the axis X, positive in the counterclockwise direction (degree or radian);

$C_{g*}(\nu)$ = the group celerity of a quasi-monochromatic wave packet of frequency ν at P_* (m/sec);

$\mathscr{E}_*(\nu,\vartheta)$ = the continuous frequency-directional energy density per unit area, per unit frequency, and per unit angle at P_* [joule/(m^2·Hz·deg)];

$\mathscr{E}_{*o}(\nu) = \int_{-\pi}^{\pi} \mathscr{E}_*(\nu,\vartheta)d\vartheta$

= the continuous frequency-directional energy density per unit area and per unit frequency at P_* [joule/(m^2·Hz)];

$\mathscr{F}_*(\nu,\vartheta) = \mathscr{E}_*(\nu,\vartheta)C_{g*}(\nu)$

= the continuous frequency-directional energy flux density across unit length, per unit time, per unit frequency, and per unit angle at P_* [joule/(m·sec·Hz·deg) = newton/deg];

$\mathscr{F}_{*o}(\nu) = \int_{-\pi}^{\pi} \mathscr{F}_*(\nu,\vartheta)d\vartheta$

= the continuous frequency-directional energy flux density across unit length, per unit time, and per unit frequency at P_* [joule/(m·sec·Hz) = newton];

$\mathscr{R}(\nu,\vartheta)$ = the wave ray of frequency ν, which passes through the point P_s at the angle ϑ relative to the positive direction of the axis X;

$P_d = \mathscr{P}_d(\nu,\vartheta)$ = the first deep water point on the backward path of $\mathscr{R}(\nu,\vartheta)$;

$A_d(\nu,\vartheta)$ = the deep water direction angle of $\mathscr{R}(\nu,\vartheta)$;

$K(\nu,\vartheta)$ = the refraction-and-shoaling coefficient (the product of refraction and shoaling coefficients) of $\mathscr{R}(\nu,\vartheta)$ at P_s relative to $\mathscr{P}_d(\nu,\vartheta)$;

<u>*3.4. Integral sea weather parameters computed via $\mathscr{E}_*$ versus integral sea weather parameters computed via $\mathscr{F}_*$*</u>

$m_{E*n}(\nu_1,\nu_2) = \int_{\nu_1}^{\nu_2} \nu^n \mathscr{E}_{o*}(\nu)d\nu$

= the nth moment of $\mathscr{E}_{o*}$ between ν_1 and ν_2;

$\nu_{E*}(\nu_1,\nu_2) = m_{E*1}(\nu_1,\ \nu_2)/m_{E*0}(\nu_1,\nu_2)$
= the mean wave frequency between ν_1 and ν_2 via $\mathcal{S}_{o*}$ (Hz);

$\tau_{E*}(\nu_1,\nu_2) = 1/\nu_{E*}(\nu_1,\nu_2)$
= the mean wave period between ν_1 and ν_2 via $\mathcal{S}_{o*}$ (sec);

$$m_{E*pq}(\nu_1,\nu_2) = \int_{\nu_1}^{\nu_2}\int_{-\pi}^{\pi} \mathcal{S}_*(\nu,\vartheta)\,|\underset{\sim}{\varkappa}_*(\nu)|^{p+q}\cos^p\vartheta\ \sin^q\vartheta d\vartheta d\nu\ :$$

$\vartheta_{E*}(\nu_1,\nu_2) = \arctan\,(m_{E*01}(\nu_1,\ \nu_2)/m_{E*10}(\nu_1,\nu_2))$
= the mean wave direction between ν_1 and ν_2 via $\mathcal{S}_*$ (radian).

The *overall mean wave frequency* $\bar{\nu}_{E*}$, *period* $\bar{\tau}_{E*}$, and *direction* $\bar{\vartheta}_{E*}$, and also the *characteristic wave height* $\bar{H}_*$, *at the point* P_* are defined *via* $\mathcal{S}_*$ by

$$\bar{\nu}_{E*} = \nu_{E*}(0,\infty),\ \bar{\tau}_{E*} = \tau_{E*}(0,\infty),\ \bar{\vartheta}_{E*} = \vartheta_{E*}(0,\infty),$$
$$\bar{H}_* = H_{*mo} = 4\sqrt{2m_{E*}(0,\infty)/(\rho g)},$$

respectively, in accordance with IAHR (1989).

Let $\gamma \in (0,\ 1]$ be a given real number, and ν_{E*M} be the frequency at which $\mathcal{S}_{o*}(\nu)$ reaches its absolute maximum. Let $\nu_{E*L}(\gamma)$ be the lowest, and $\nu_{E*G}(\gamma)$ be the greatest frequency with the property that

$$\mathcal{S}_{o*}(\nu_{E*L}(\gamma))/\mathcal{S}_{o*}(\nu_{E*M}) = \mathcal{S}_{o*}(\nu_{E*G}(\gamma))/\mathcal{S}_{o*}(\nu_{E*M}) = \gamma.$$

Then the *overall centroidal γ-peak wave frequency* $\hat{\nu}_{E*}$, *period* $\hat{\tau}_{E*}$, and *direction* $\hat{\vartheta}_{E*}$ *at the point* P_* are defined *via* $\mathcal{S}_*$ by

$$\hat{\nu}_{E*} = \nu_{E*}(\nu_{E*L}(\gamma),\nu_{E*G}(\gamma)),\ \hat{\tau}_{E*} = \tau_{E*}(\nu_{E*L}(\gamma),\nu_{E*G}(\gamma)),$$
$$\hat{\vartheta}_{E*} = \vartheta_{E*}(\nu_{E*L}(\gamma),\nu_{E*G}(\gamma)),$$

respectively. In this study, we have set $\gamma = 0.8$, in accordance with IAHR (1989).

All the above definitions of this subsection, except for the definition of '$\bar{H}_*$', apply with 'F' and '$\mathcal{F}$' in place 'E' and '$\mathcal{S}$', respectively.

3.5. Parameters characterizing discrete spatiotemporal Fourier transform of the sea surface displacement from equilibrium at the point P_*

ν_m = the low cutoff wave frequency (Hz);

ν_M = the high cutoff wave frequency (Hz);

I = the total number of discrete frequencies in the interval $[\nu_m, \nu_M]$;

$\Delta\nu$ = the wave frequency increment (Hz);

$f(i) = \nu_m + (i - 1)\Delta\nu$

= the discrete wave frequency of index $i \in \langle 1, 2, \ldots, I \rangle$;

ϑ_{*m} = the least (low cutoff) wave ray direction angle at the point P_* (radian or degree);

ϑ_{*M} = the greatest (high cutoff) wave ray direction angle at the point P_* (radian or degree);

J_* = the total number of discrete wave ray direction angles in the interval $[\alpha_{*m}, \alpha_{*M}]$;

$\Delta\vartheta_*$ = the shallow water wave ray direction angle increment (radian or degree);

$\vartheta_*(j) = \vartheta_{*m} + (j - 1)\Delta\vartheta_*$

= the wave ray direction angle of index j at the point P_* relative to the positive direction of the X-axis (radian or degree);

$E_*(i, j) = \mathcal{E}_*(f(i), \vartheta_*(j))\Delta\nu\Delta\vartheta$

= the discrete energy density of indices i and j per unit area at P_* (joule/m^2).

$F_*(i, j) = F_*(f(i), \vartheta_*(j))\Delta\nu\Delta\vartheta$

= the discrete energy flux density of indices i and j across unit length and per unit time at P_* [joule/(m·sec) = newton/sec].

4. Expressions for the frequency-directional energy density and energy flux density in deep water in terms of those in shallow water

The general idea of how to express E_d or F_d in terms of the respective E_s or F_s, is based on this hypothesis:

Hypothesis 1: [*During a storm caused by a distant source,*] *the wave pattern in deep water is statistically* *(ergodically) uniform over an area of the sea surface whose linear dimensions are small as compared to the distance from the storm source.*

The most important *specific* factors which influence the character most frequency-directional spectra of sea waves during the winter storms off the Mediterranean coast of Israel are (i) a single narrow window for deep water wave approach and (ii) a fetch of approximately 2200–2300 km in length (see Goldsmith & Golik (1978, p. 22), Carmel *et al* (1985a, 1985b). We therefore adopt the following hypothesis:

Hypothesis 2: [*During a storm caused by a distant source,*] *for each point* P_* *along the Mediterranean coast of Israel, the spatiotemporal discrete Fourier decomposition of the sea surface displacement during an FME contains exactly one plane monochromatic wave whose direction is uniquely determined by its frequency.*

To be able to analyze all available data uniformly, we have, in accordance with common practice, extended Hypotheses 1 and 2 by omission of the phrase enclosed between square brackets. Thus, by Hypothesis 2, for each for FME, each $i \in \{1,2,\ldots, I\}$, there is exactly one $j \in \{1,2,\ldots, J_*\}$ such that $\theta_*(i) = \vartheta_*(k_*(i))$, i.e. $\theta_* = \vartheta_* \circ k_*$, where k_* is a certain integer-valued function of an integer argument, and θ_* is a composite real-valued function defined herewith. Hence,

$$E_*(i,j) = E_{o*}(i)\delta_{j,k_*(i)}, \quad E_{o*}(i) = \sum_{j=0}^{J_*} E_*(i,j), \tag{1}$$

where δ is the unit diagonal matrix. By Hypothesis 1, we then have

$$E_{od}(i) = E_{os}(i)[K(f(i),\theta_s(i)]^{-2}, \tag{2}$$

$$\theta_d(i) = A_d(f(i),\theta_s(i)). \tag{3}$$

By the respective definitions of Sections 3.3, and 3.5, the variant of (1) with 'F' in place of 'E' is semantically sound. Under Hypothesis 2, equations (2) and (3) solve the problem of expressing E_d in terms of E_s, whereas $F_d = E_d C_{gd}$ and $F_{do} = E_{do} C_{gd}$.

5. Data processing

Broadly speaking, the data processing underlying this study comprises four steps.

1). The first step of data processing was accomplished with the aid of a package of original FORTRAN programs recently developed by Iosilevskii & Iosilevskii (1991). At this step, each time series of raw shallow water pressure data, gathered by each wave measuring station during the corresponding *FME* was tested on reliability in accordance with certain criteria, and, if reliable, it was Fourier transformed with the purpose to obtain the respective table $\langle f, E_{0s}, F_{0s}, \theta_s \rangle$. Among some other results, the programs also compute the cumulative longshore energy density flux across unit length over any given span of time; such a flux is commonly associated with the respective longshore sediment transport.

2). The second step of the data processing was accomplished with the aid of *Multi-frequency and multi-ray FORTRAN program for backward and forward refraction of water waves* (briefly, *BFRFP*) recently written by Iosilevskii (1992). Using the bottom topography data for the neighborhood of the wave measuring station, the program computes, among some other wave ray parameters, the *matrix* A_d *of deep water wave propagation angles* and the *matrix* K *of products of refraction and shoaling coefficients*. The size $I \times J_s$ of each matrix is specified by the user of the program. Once computed, the matrices A_d and K become *universal* attributes of the neighborhood of the wave measuring station independent of any specific wave weather or wave climate.

In this study, we have used the following values:

$$\nu_m = 6.0 \times 2^{-10} \text{ Hz}, \; \nu_M = 0.25 \text{ Hz}, \; \Delta\nu = 1024^{-1} \text{ Hz},$$
$$\vartheta_{sm} = -45^\circ, \; \vartheta_{sM} = 45^\circ, \; \Delta\vartheta_s = (90/89)^\circ,$$
$$I = 251, \; J_s = 90.$$

3). The third step of the data processing was accomplished with the aid of *Deep water spectrum FORTRAN program* (briefly, *DWSFP*) which was recently written by Ya.A.Iosilevskii (to be published). At the first place, the program transforms a sequence of tables $\langle f, E_{0s}, F_{0s}, \theta_s \rangle$, obtained at the first step, into the respective sequence of tables $\langle f, E_{0d}, F_{0d}, \theta_d \rangle$. This is done with the aid of the matrices A_d and K obtained at the second step. Then using E_{s0}, F_{s0}, E_{d0}, and F_{d0} as statistical weights, the program computes, for each individual FME, the following mean and peak sea state parameters:

$$E_{so} \rightarrow \bar{H}_s,\ \bar{\tau}_{Es},\ \bar{\vartheta}_{Es},\ \hat{\tau}_{Es},\ \hat{\vartheta}_{Es}; \tag{4}$$

$$F_{so} \rightarrow \bar{\tau}_{Fs},\ \bar{\vartheta}_{Fs},\ \hat{\tau}_{Fs},\ \hat{\vartheta}_{Fs}; \tag{5}$$

$$E_{do} \rightarrow \bar{H}_d,\ \bar{\tau}_{Ed},\ \bar{\vartheta}_{Ed},\ \hat{\tau}_{Ed},\ \hat{\vartheta}_{Ed}; \tag{6}$$

$$F_{do} \rightarrow \bar{\tau}_{Fd},\ \bar{\vartheta}_{Fd},\ \hat{\tau}_{Fd},\ \hat{\vartheta}_{Fd}. \tag{7}$$

Most of the parameters listed in (4) and (5) are also computed by the programs used at step 1. The parameters listed (6) and (7) are the desired deep water sea state parameters computed by the *spectral decomposition method*.

$\bar{H}_s$, $\bar{\tau}_{Es}$, and $\bar{\vartheta}_{Es}$ can be regarded as the wave height, period, and propagation vector direction of an imaginary monochromatic wave at the point P_s, and $\bar{H}_s$, $\bar{\tau}_{Fs}$, and $\bar{\vartheta}_{Fs}$ as the similar characteristics of another imaginary monochromatic wave. With the aid of the appropriate matrix elements of the matrices A_d and K, the program computes the deep water wave heigth $\bar{H}'_{Ed}$ and direction $\bar{\vartheta}'_{Ed}$ corresponding to the triple $\langle\bar{H}_s,\ \bar{\tau}_{Es},\ \bar{\vartheta}_{Es}\rangle$, and it also computes the similar characteristics $\bar{H}'_{Fd}$ and $\bar{\vartheta}'_{Fd}$ corresponding to the triple $\langle\bar{H}_s,\ \bar{\tau}_{Fs},\ \bar{\vartheta}_{Fs}\rangle$.

$\bar{H}'_{Ed}$, $\bar{\tau}_{Es}$, and $\bar{\vartheta}'_{Ed}$ are conventional deep water characteristics of sea state computed in the framework of the presently common *representative monochromatic wave method*. $\bar{H}'_{Fd}$, $\bar{\tau}_{Fs}$, and $\bar{\vartheta}'_{Fd}$ form a similar set of deep water sea state parameters, but this set is not in common usage - it is suggested here for the first time.

4). The fourth step of the data processing comprises statistical analysis and graphic and table presentation of the results obtained. The statistical analysis was done with the aid of programs prepared by the second author. The graphic and table presentation was done with the aid of Quattro Pro Software of Borland Intl.

6. Results

The results of this study can be summarized as follows.

1). There is both deterministic and statistical correlation between the deep water sea weather parameters at Haifa and of the respective parameters at Ashkelon, with the exception of the directional parameters. The latter parameters are correlated statistically and, to a lesser extent, mainly during storms, they are also correlated deterministically.

2). **The prevailing wave direction is from West-North-West at Haifa, and it is from West at Ashkelon.**

3). For the same place (Haifa or Ashkelon), there is deterministic and statistical correlation between the deep water sea weather parameters computed via E_{do} and the respective parameters computed via F_{do}. In this case, the values of '$\bar{\tau}_{Ed}$' and '$\hat{\tau}_{Ed}$' sometimes differ from the respective (simultaneous) values of '$\bar{\tau}_{Fd}$' and '$\hat{\tau}_{Fd}$', whereas $\bar{\vartheta}_{Ed}$ and $\hat{\vartheta}_{Ed}$ are, as a rule, close to $\bar{\vartheta}_{Fd}$ and $\hat{\vartheta}_{Fd}$, respectively.

4). There is both deterministic and statistical correlation between values of the deep water sea weather parameters computed by the spectral decomposition method and the respective parameters computed by the representative monochromatic wave method, although during a storm the former values seem to be more stable (more smooth) in time than the latters.

5). Comparison of the present estimates of the prevailing wave direction at Ashkelon, based on *instrumental* measurements, with the previous estimates of the prevailing wave direction at Ashdod (Rosen (1982)), 15 km North of Ashkelon, based on *visual observations*, shows that the two estimates are grossly different.

Some of the results of this study are illustrated in Figures 1 - 6.

Acknowledgements

The research underlying this paper was partly sponsored by the Agency for International Development, U.S.A. BFRFP was written by Ya.A.Iosilevskii under the sponsorship of Israeli Ministry of Energy and Infrastructure. The authors thankfully acknowledge the sponsorship of the above two bodies.

The bathymetry survey to collect the raw data for preparing the two depth grids covering wide regions off Haifa and off Ashkelon along the Mediterranean coast of Israel, where our CAS wave measuring stations are located, was made by Mr. G.Amit and by Mr. A.Golan who also prepared the grids. Mr. P.Artsztein and Mr. A.Cohen digitalized the continuous bathymetric records. Mr. G.Amit and Mr. D.Ramot maintained the wave measuring equipment. The authors are deeply indebted to all the above persons for their cooperation.

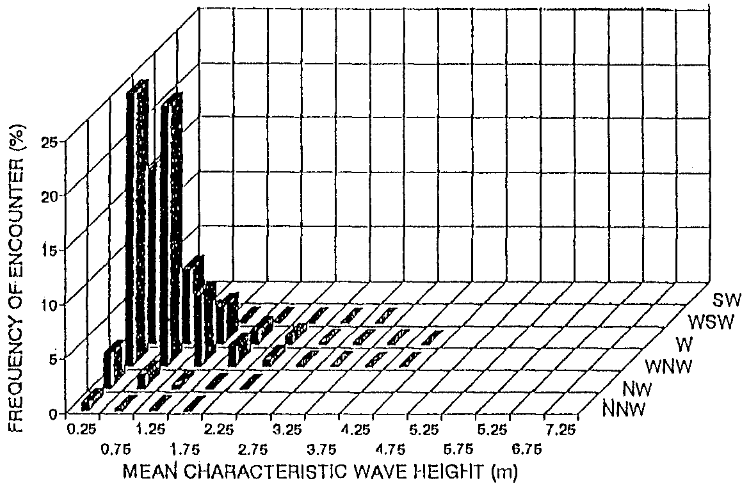

Fig. 1. The yearly deep water wave direction distribution off Haifa (Dado Beach) in 1984 - 1991

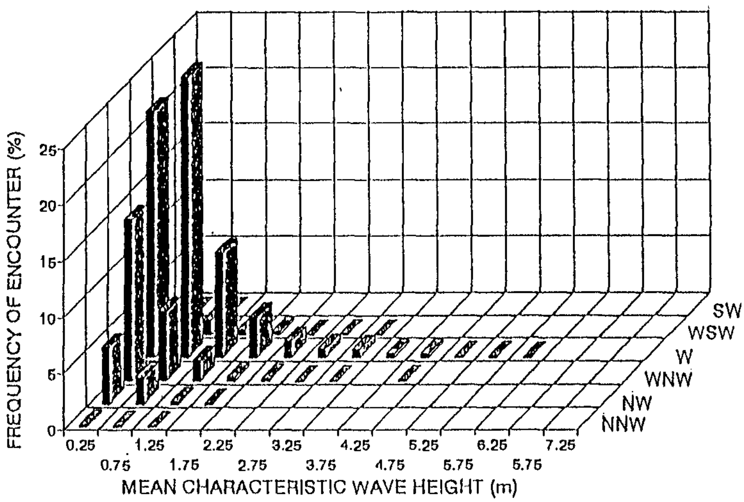

Fig. 2. The yearly deep water wave direction distribution off Ashkelon in 1984 - 1990

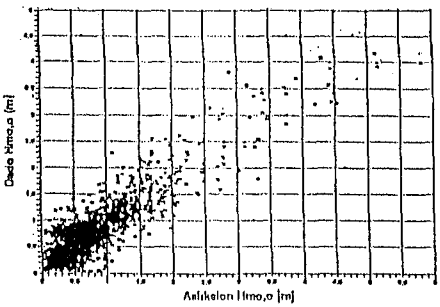

Fig. 3. Comparison of the deep water wave heights $(\bar{H}_d)$ off Haifa (Dado Beach) and that off Ashkelon in 1984 - 1990

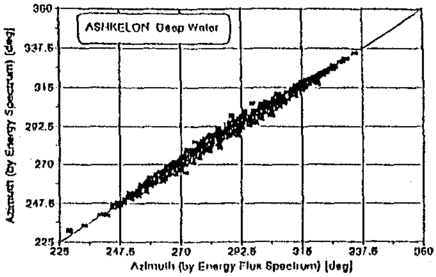

Fig. 4. Comparison of the mean deep water wave directions computed via energy density and those computed via energy density flux; Ashkelon; 1984 - 1990

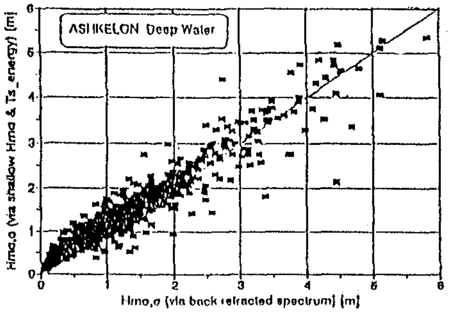

Fig. 5. Comparison of the mean deep water wave heights computed by the spectral decomposition method $(\bar{H}_d$, the abscissa axis) and those computed by the representative monochromatic wave method $(\bar{H}'_{Ed}$, the ordinate axis); Ashkelon, 1984 - 1990

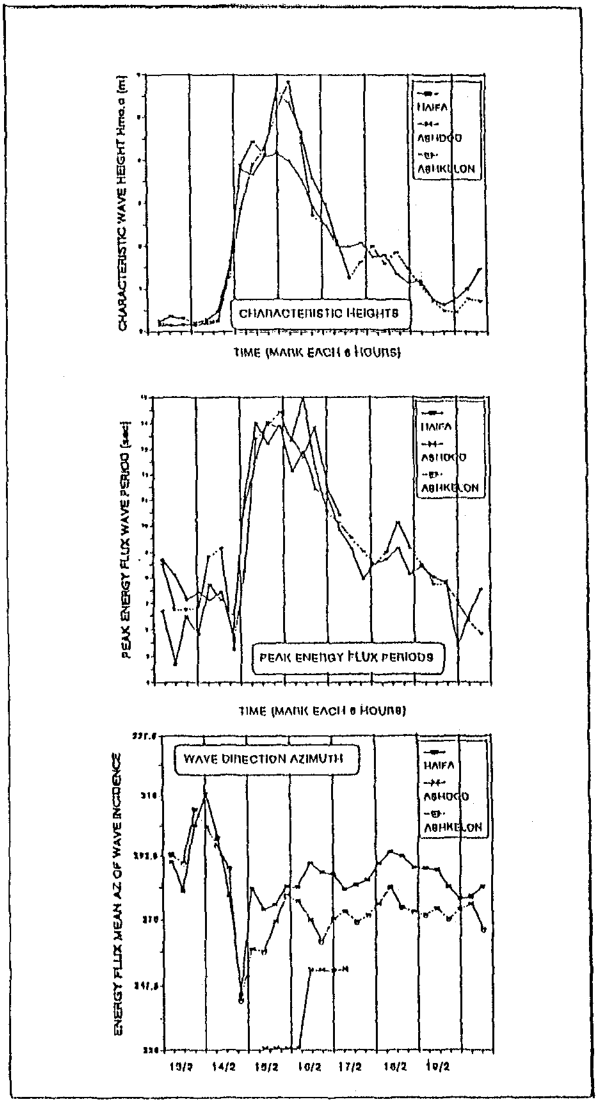

Fig. 6. Comparison of the deep water storm patterns off Haifa (this study), Ashkelon (this study), and Ashdod (visual observations), 13-19 February 1985

Appendix I. References

Boyd, W., and Lowe R. L. (1985). "A high density cassette data acquisition system." *Ocean*, 85, v.1, 606-609.

Carmel L, Z., Inman, D. L., and Golik A., (1985a). "Characteristics of storm waves off the Mediterranean coast of Israel." *Coastal Eng.*, 9, 1-19.

Carmel L, Z., Inman, D. L., and Golik A., (1985b). "Directional wave measurements at Haifa, Israel, and sediment transport along the Nile Littoral Cell." *Coastal Eng.*, 9, 21-36.

Goldsmith V., and Golik A. (1978). *The Israeli wave climate and logshore sediment transport model.* IOLR Geological Department Report No 78/1, Haifa, Israel. 56 pp. + Appendices A-C.

Goldsmith V., and Sofer S. (1983). "Wave climatology of the Southeastern Mediterranean." *Israel Journal of Earth-Sciences*, 32, 1-61.

IAHR (1989). "List of sea-state parameters." *J. Wtrwy., Port, Coast, and Oc. Engrg.*, ASCE, 115(6), 293-808.

Iosilevskii Ya. A., and Iosilevskii G. (1991). *FORTRAN programs for directional spectral analysis of water wave data from a CAS station.* IOLR Report H23/91, Haifa, Israel, 36 pp. + Appendices A-E.

Iosilevskii Ya. A. (1992). *Multi-frequency and multi-ray FORTRAN program for backward and forward refraction of water waves.* IOLR Report H15/92, Haifa, Israel. 212 pp. 212.

Rosen, D. S. (1982). *A new deep water wave climate evaluation for Ashdod.* Technical Report P. N. 100/82. Technion, Haifa, Israel, 99 pp.

Rosen, D. S., and Kit, E. (1981). "Evaluation of the wave characteristics at the Mediterranean coast of Israel." *Israel Journal of Earth-Sciences*, 30, 120-134.